Improved Model to Predict Properties of Aluminum Alloy Products after Continuous Cooling

J.T. STALEY, R.D. DOHERTY, and A.P. JAWORSKI

Previous models of quench sensitivity of age-hardening alloys have been extended to include loss of toughness as well as loss of yield strength upon postquench aging. Loss of toughness on slow quenching was modeled by the loss of solute to grain-boundary precipitates that promote intergranular fracture. The phenomena are modeled using differential equations, and the model includes temperature-dependent values of the minimum toughness and strength expected after extended isothermal hold times. Time-temperature-property (TTP) curves for the postaging yield strength and toughness were used to provide empirical kinetic and property data for fitting the proposed relationship. The model was tested against experimental data, both nominally isothermal and truly continuous cooling, for an Al-Cu-Li alloy plate. For nominally isothermally cooling, the model proved to be capable of accurately describing the loss of toughness and the loss of strength to a much larger loss in strength than previous models. The model also successfully predicted the loss of strength on continuous cooling but provided a conservative overestimate of the loss of toughness under the same continuous-cooling conditions. It is suggested that this bias arises from the lack of consideration of differences in the microstructure of the precipitates formed during isothermal treatments and those formed during continuous cooling.

I. INTRODUCTION

ALL precipitation-hardenable–aluminum alloy products progressively lose their ability to develop the maximum strength attainable with a particular aging treatment as rate of cooling from the solution temperature decreases. This quench sensitivity is attributed to loss of solute by precipitation during the quench as coarse, heterogeneously nucleated particles of the equilibrium phase and to loss of vacancies to sinks.

Cahn has shown that kinetics of continuous transformation can be predicted using isothermal transformation kinetics.[1] His approach was modified to predict the ability of precipitation-hardenable–aluminum alloy products to develop strength after continuous cooling.[2] The model has been improved and implemented over the years.[3] The inputs are a time-temperature-property (TTP) C-curve analogous to a time-temperature-transformation (TTT) C-curve and a measured or postulated time-temperature cooling curve (quench curve). In the usual implementation of the model, the C-curve is described mathematically using constants determined by regression analysis of data obtained from isothermal quenching experiments. The C-curve equation, Eq. [1], is given in terms of empirically determined constants, K_2 to K_5, but uses a form based on the accepted theory of nucleation.[4]

$$C_t(T) = k_2 \exp\left(\frac{k_3 k_4^2}{RT(k_4 - T)^2}\right) \exp\left(\frac{k_5}{RT}\right) \qquad [1]$$

where $C_t(T)$ = critical time at temperature T for attainable strength σ;
k_2 = constant which includes the reciprocal of number of potential nucleating sites;
k_3 = constant which includes the change in free energy associated with formation of a nucleus;
k_4 = constant related to solvus temperature;
k_5 = mobility term; and
R = gas constant.

To describe a particular level of σ, another term, k_1, is added:

$$C_t(T)_x = k_1 k_2 \exp\left(\frac{k_3 k_4^2}{RT(k_4 - T)^2}\right) \exp\left(\frac{k_5}{RT}\right) \qquad [2]$$

where $C_t(T)_x$ = critical time to decrease attainable strength σ to a level where σ equals σ_x;
$k_1 = -\log_e (\sigma_x - \sigma_{min}/\sigma_{max} - \sigma_{min})$;
σ_x = usually chosen to equal 0.995 σ_{max};
σ_{max} = maximum level of σ; and
σ_{min} = minimum level of σ.

To simplify the mathematics in the original version of the model, an approximation was made that strength after infinitely long hold times at temperatures below the solvus, σ_{min}, would equal zero. This model was able to predict loss in strength accurately for those quench paths which result in a loss of up to about 0.1 σ_{max}. In a subsequent version of the model, a better approximation was made which assumed that σ_{min} is a constant that is independent of temperature.[5] Predictions with this model were useful to losses of about 0.15 of σ_{max}.

II. NEW MODEL

This article describes a new model which recognizes that σ_{min} is a function of temperature. The model is developed on a sounder mathematical basis and increases the capability to predict strength to much lower percentages of σ_{max}. The new model is, however, still based

J.T. STALEY, Corporate Consultant, and A.P. JAWORSKI, Staff Scientist, are with Alcoa Technical Center, Alcoa Center, PA. R.D. DOHERTY, Professor, is with Drexel University, Philadelphia, PA.
Manuscript submitted October 2, 1992.

on some assumptions which are described later. Moreover, the format permits easy implementation into more general models depicting the role of metallurgical factors on the structure and properties of aluminum alloys due to thermomechanical processing.

The model assumes that the rate of loss of solute during quenching is a first-order reaction. The assumption has been largely verified by various empirical studies.[2,3,5] The phenomenon is described by a differential equation:

$$\frac{ds}{dt} = -A(T)\,(s - s_{\min}(T)) \qquad [3]$$

where s = concentration of solute in solution;
t = time at temperature, T;
$A(T)$ = kinetic constant; and
$s_{\min}(T)$ = equilibrium solute concentration at T.

Based on the assumption that attainable yield strength depends linearly on solute concentration, one can rewrite Eq. [2] as follows:

$$\frac{d\sigma}{dt} = -k(T)(\sigma - \sigma_{\min}(T)) \qquad [4]$$

For constant temperature, integration of this equation gives

$$\sigma = \sigma_{\min}(T) + (\sigma_{\max} - \sigma_{\min}(T)) \exp(-k(T)t) \qquad [5]$$

where σ = strength capability after time t at temperature T;
$\sigma_{\max}$ = maximum value of σ;
$\sigma_{\min}(T)$ = minimum value of σ at temperature T; and
$k(T)$ = kinetic constant at temperature T.

It is shown rigorously in Appendix A that for continuous cooling, the term $k(T)$ can be replaced by

$$k(T) = \left(\frac{1}{C_t(T)}\right) \qquad [6]$$

where $C_t(T)$ is as defined in Eq. [1].

This leads to the following equation which describes the attainable property after cooling over any path:

$$\frac{d\sigma}{dt} = -\frac{1}{C_t(T)}(\sigma - \sigma_{\min}(T)) \qquad [7]$$

A model was also developed to predict the ability to develop toughness on aging after continuous cooling. This model is based on the observation that postaged toughness falls as the percentage of intergranular fracture increases due to an increase in grain-boundary precipitates formed by precipitation of solute during cooling. The fall of toughness over a small temperature interval can be predicted from the simultaneous loss in strength scaled by the maximum possible loss in toughness ($K_{\max} - K_{\min}(T)$) that can occur during isothermal holding. The model assumes that the effects of the morphology of the precipitates, which serve to decrease toughness by increasing the proportion of intergranular fracture, are accounted for by the loss of toughness determined empirically by isothermal quenching experiments and, therefore, contains no terms which represent microstructure. In the previous model, the equation for K was expressed as a function of time.[6,7] For the current model, a differential equation was developed:

$$\frac{dK}{dt} = -\frac{1}{D_t(T)}(K_{\max} - K_{\min}(T))\left[\frac{\sigma - \sigma_{\min}(T)}{\sigma_{\max} - \sigma_{\min}(T)}\right]^{C_t(T)/D_t(T)} \qquad [8]$$

where K = measure of fracture toughness;
$K_{\max}$ = toughness with maximum quench rate; and
$K_{\min}(T)$ = minimum value of toughness at temperature T;

and

$$D_t(T) = m_2 \exp\left(\frac{k_3 k_4^2}{RT(k_4 - T)^2}\right) \exp\left(\frac{k_5}{RT}\right) \qquad [9]$$

where $D_t(T)$ = critical time at temperature T for attainable toughness; and
m_2 = constant which includes reciprocal of number of potential nucleating sites of precipitates which influence K.

The derivation of Eq. [8] is presented in Appendix B.

III. VERIFICATION OF THE MODEL

The model was tested using data from a previous investigation. Full experimental details have been previously published.[6,7] Briefly, panels taken from the midplane of an experimental alloy plate containing 2.7 pct Cu, 1.6 pct Li, 0.09 pct Zr, 0.05 pct Fe, 0.05 pct Si, and 0.10 pct Ti were quenched from the solution heat-treatment temperature into molten metal baths at five temperatures ranging from 250 °C to 450 °C (523 to 723 K), held for a series of times, then quenched to room temperature. The experimental cooling curves of these samples were measured by embedded thermocouples at the sample's midthickness. Because of the lower conductivity of Al-Li alloy products compared to that of standard aluminum alloy products, there was a significant delay, from 15 to 20 seconds, before the sample cooled to within 10 °C of the isothermal hold temperature and hundreds of seconds before the temperature was within 1 °C.[7] The nonisothermal parts of the nominally isothermal treatments were used in the modeling procedure discussed later. For simplicity, the nominally isothermal treatment will be referred to as isothermal treatment for the remainder of this article, even though samples held for the shorter times were more than 10 degrees hotter than the bath temperature at the time of their removal, and few of the samples attained a temperature within one degree of bath temperature.

The phases present in the isothermally treated specimens were determined using X-ray diffraction analyses and their preferred nucleation sites were determined using

transmission electron microscopy of specimens treated at 673, 623, and 573 K.

Six other panels were continuously cooled from the solution heat-treatment temperature to produce a number of quench paths. All panels were stretched 6 pct and then artificially aged 24 hours at 436 K. A longitudinal-tension specimen and a L-T compact toughness specimen were removed from each panel and tested. The K value at 10 pct offset was used as a criterion of fracture toughness and was designated KR_{10}. Fracture characteristics were related to microstructural features by preparing fractured toughness specimens in such a way that both a polished and etched surface and the fractured surface could be examined simultaneously in a scanning electron microscope.

IV. RESULTS AND DISCUSSION

A. *Isothermal Treatments*

The X-ray diffraction analyses indicated that the T_1 phase (Al_2CuLi) precipitated at a slightly higher rate at temperatures above about 623 K while the T_B phase (Al_7Cu_4Li) precipitated at a higher rate at lower temperatures. Transmission electron microscopy revealed that the T_B phase nucleated almost exclusively within the grains and grew as rod-shaped particles. Many of the T_B precipitates nucleated on triangular-shaped particles containing silicon which were invariably associated with Al_3Zr dispersoid particles.[8] Some Θ' particles (Al_2Cu), which nucleated in the matrix, were observed in the specimens exposed at 573 K. In contrast, T_1 phase nucleated mainly on grain boundaries at shorter times and on subgrain boundaries after longer times. The particles grew as long, thin plates which puckered the grain boundaries as observed by Tosten *et al.*[9] The number density increased and plate size decreased with decreasing temperature. With even longer times, T_1 platelets nucleated in the matrix and grew.

Strength and toughness of the aged material decreased monotonically with increasing hold time, then asymptotically approached values which were temperature dependent. Both strength and toughness decreased most rapidly at 623 K and reached their lowest values at this temperature also. The loss in toughness at a particular yield strength was highly dependent on the isothermal hold temperature, as shown in Figure 10 which was obtained by cross plotting the fitted results. Material exposed at 623 K developed the lowest toughness when compared at any yield strength.

The initial minimum strength decreased with decreasing isothermal hold temperature to 623 K followed by an increase in minimum strength at lower temperatures. This can be readily explained. The minimum strength attained after holding for long times at each temperature decreased with decreasing temperature to 623 K because the T_1 and T_B precipitated in a size which did not contribute to strength. Therefore, strength after aging was simply a function of the solute remaining in solution after the quench from the hold temperature. The minimum attainable strength after holding below 623 K was higher, however, because the Θ' precipitates within the grains were fine enough to provide some strengthening. This strengthening was additive with that developed during aging.

Effects of isothermal hold temperature on microstructural features and resulting fracture characteristics and toughness can be summarized as follows. Direct-quenched material fractured by transgranular-ductile rupture initiated by coarse intermetallic particles of Al_7Cu_2Fe which formed during ingot solidification. After short exposure times at any temperature, fracture toughness fell because T_1 plates along grain boundaries nucleated fracture at grain boundaries (Figure 1). The areas of intergranular fracture were connected by transgranular tearing. With longer times at intermediate temperatures, T_1 precipitated on subgrain boundaries and within the grains, and a small amount of T_B precipitated in the matrix on dispersoid particles. The T_1 platelets on subgrain boundaries caused fracture along the subgrain boundaries. This made fracture easier than by transgranular tearing, so toughness decreased (Figure 2). Toughness dropped to a lower level in material treated at 623 K than at higher temperatures because T_1 was more closely spaced along the boundaries. At lower temperatures, T_1 also

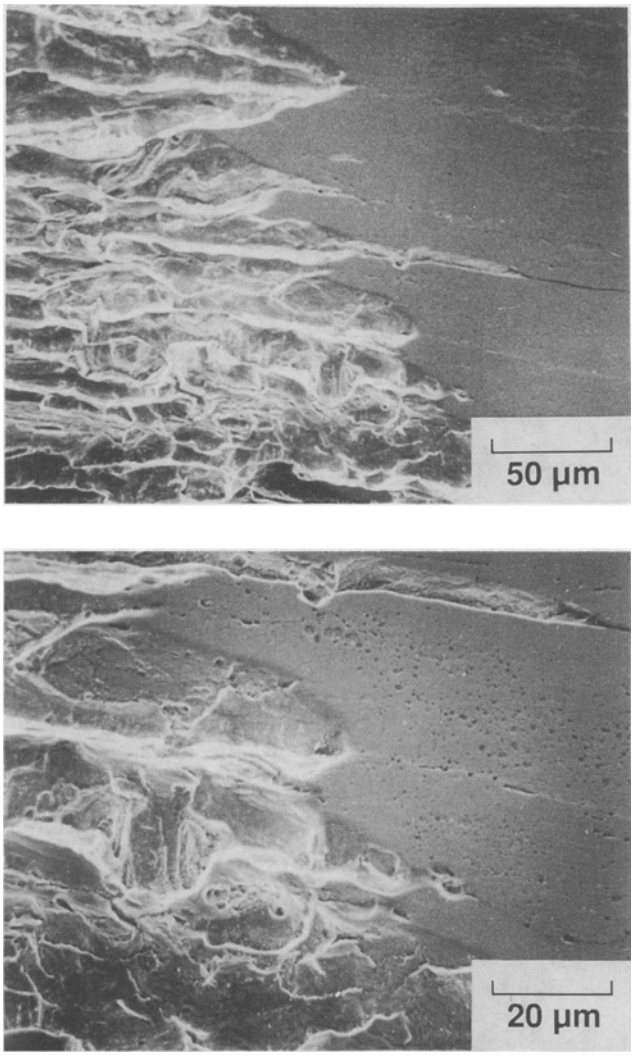

Fig. 1—Combination fractograph-micrographs of material held 10 s at 350 °C illustrate that fracture is influenced by grain boundaries but also fractures across grains.

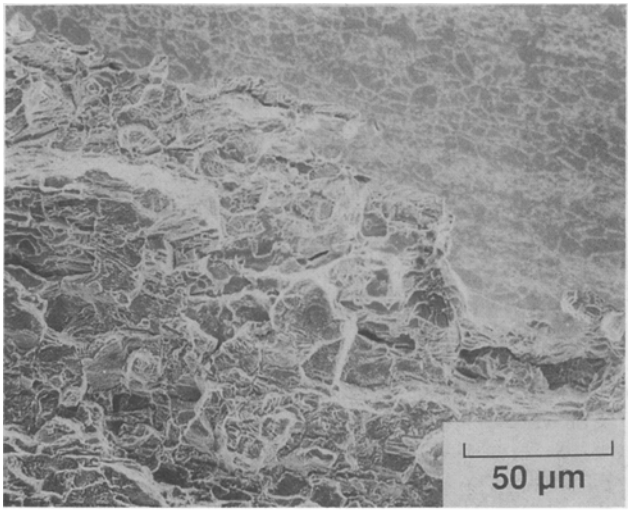

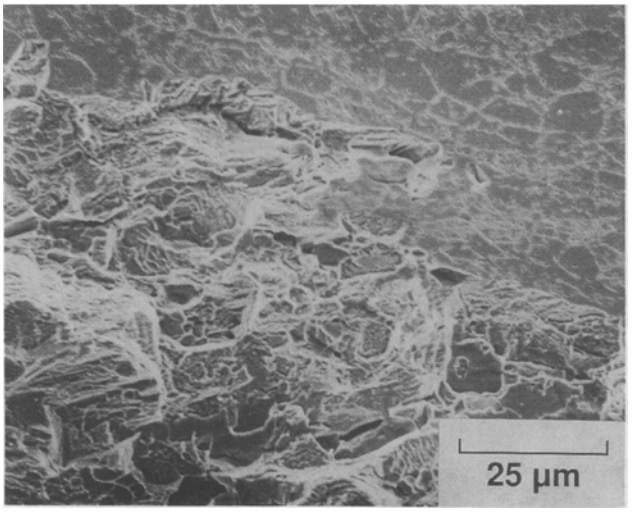

Fig. 2—Combination fractograph-micrographs of material held 100 s at 350 °C illustrate that fracture follows grain and subgrain boundaries.

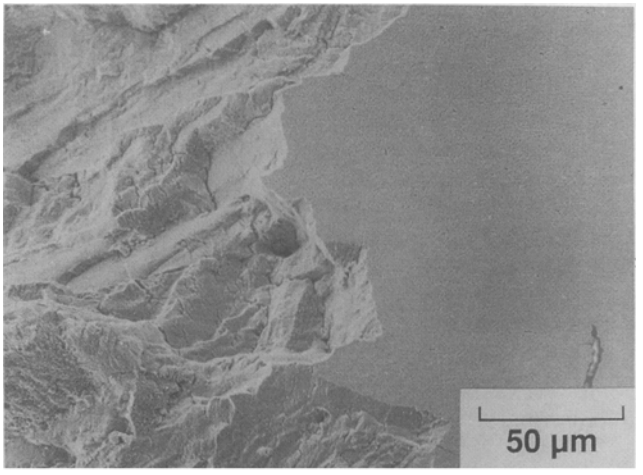

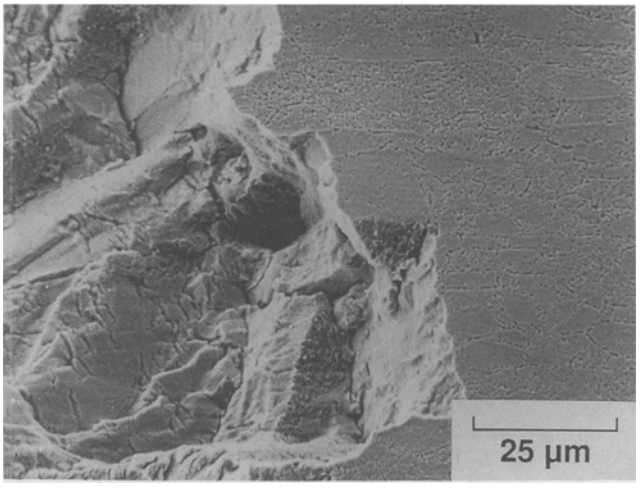

Fig. 3—Combination fractograph-micrographs of material held 300 s at 300 °C illustrate that fracture is influenced by subgrain boundaries but is highly transgranular.

precipitated on boundaries, but matrix precipitation of T_B was favored over precipitation of T_1 and some Θ' precipitated in the matrix. Consequently, fracture occurred both along grain and subgrain boundaries and across the grain (Figure 3). For a particular loss in strength, the amount of T_1 on boundaries decreased with decreasing temperature, so toughness loss was less than that occurring near 623 K. With longer times at the higher temperatures, T_1 platelets coarsened to such an extent that their nucleation sites could not be clearly identified. Fracture path was highly influenced by the platelets. The scale of the changes in fracture path (Figure 4) agrees with that of the precipitate spacing.

The cooling curves of the isothermally quenched panels and their tensile yield strengths and 10 pct secant offset values from R curves, KR_{10}, were used to determine the values of the constants in Table I from which TTP curves for tensile yield strength and KR_{10} fracture toughness were derived. Parameters from empirical relationships which describe the effect of temperature on the terms σ_{min} and K_{min} were also estimated. Inspection suggested that the effect on tensile yield strengths could be described by a parabola, so $\sigma_{min}(T)$ was set equal to $b_0 + b_1T + b_2T^2$. When this relationship predicted values above that of σ_{max}, σ_{min} was set equal to σ_{max}. To determine the parameters for the KR_{10} C-curve, the procedure was different. Two converging straight lines best described the effect of temperature on $K_{min}(T)$ for KR_{10}, so the following was used:

Condition	$K_{min}(T)$
$T \leqq 633$ K	$c_0 + c_1T$
$T \geqq 633$ K	$d_0 + d_1T$

Because the fundamental factors affecting the terms k_3 to k_5 were believed to be the same for the C-curves of yield strength and toughness, these parameters were estimated using a procedure which included both yield strength and KR_{10} values in the same analysis. The other parameters, however, were estimated by considering strength and toughness indicators separately.

The data set consisted of a series of N groups (cooling curve, measured property value). The estimation procedure is outlined as follows:

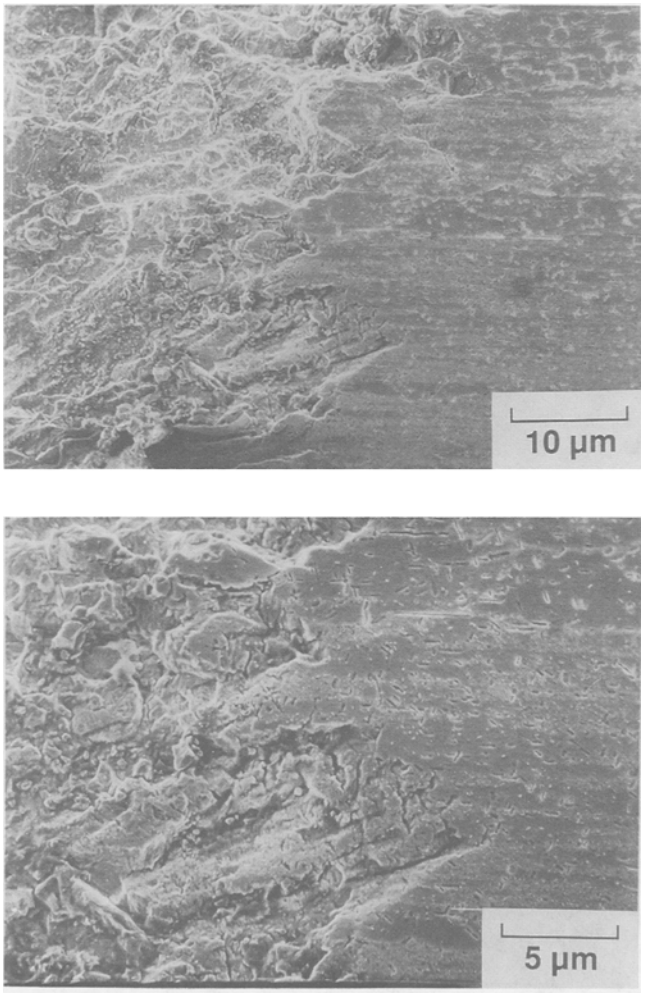

Fig. 4—Combination fractograph-micrographs of material held 300 s at 400 °C illustrate that fracture is influenced by precipitate plates.

(a) Guess a value for each parameter.
(b) Predict a strength and KR_{10} value for each data group by solving Eqs. [8] and [9] for each cooling curve.
(c) Compute the values of the following objective functions:

$$SS = SS_1 + SS_2$$

where

$$SS_1 = \sum_{j=1}^{N} (\sigma_j - \hat{\sigma}_j)^2$$

where σ_j = measured strength value for the jth data set and
$\hat{\sigma}_j$ = corresponding predicted value;

and

$$SS_2 = 10 \sum_{j=1}^{N} (K_j - \hat{K}_j)^2$$

where K_j = measured toughness value for the jth data set and
$\hat{K}_j$ = corresponding predicted value.

(d) Check convergence.
(e) Adjust the parameters if necessary and go to step (b).

Equations [7] and [8] were solved using an ordinary differential equation solver, in particular, the LSODA code from ODEPACK, software developed at the Lawrence Livermore Laboratory, Livermore, CA.[10] Parameter estimates (step e) were done using the N2SOL procedure.[11] The best estimates of the values of the parameters are presented in Table I.

The TTP C-curve for 99.5 pct of maximum yield strength is plotted in Figure 5 along with similar C-curves for alloys 7075-T6,[2] 7050-T76,[2] 2024-T8,[5] and 2219-T8.[12] The C-curves for a series of values of yield strength and KR_{10} fracture toughness are presented in Figures 6 and 7. The sharp knee in Figure 7 is considered to be an artifact attributed to the use of two straight lines to represent K_{min}.

The relative goodness of fit compared to previous methods which considered σ_{min} and K_{min} to equal either zero or a constant was analyzed using the residual sum of squares divided by the approximate number of degrees of freedom (RSS/DF), as shown in the following:

	RSS/DF
$\sigma_{min} = 0$	2761
σ_{min} is a constant	98
σ_{min} is $f(T)$	68
$K_{min} = 0$	59
K_{min} is a constant	16
K_{min} is $f(T)$	9

The advantage of the new model is apparent. As illustrated in the plot of calculated *vs* measured values of yield strength in Figure 8, values as low as 50 pct of maximum were successfully fitted.

B. *Continuously Cooled*

The model using the constants in Table I, obtained from the isothermal studies, was applied to the continuously cooled samples. Due to the nature of the σ_{min} and K_{min} dependence on temperature, at some point on the σ or K trajectory, one may encounter a situation when the current property value will be equal to its corresponding minimum value. A further drop in temperature would result in a negative $(\sigma - \sigma_{min})$ or $(K - K_{min})$ driving force. This would formally lead to the sample regaining some of the lost strength or toughness. This situation has no physical justification, so at any time during the integration of Eqs. [6] and [7] the negative driving force occurs, the appropriate time derivative was set to zero to prevent this from occurring.

The ability of the model to fit the data for the yield strengths of the isothermally quenched materials and to predict the yield strengths of the continually cooled samples is illustrated in Figure 8. The model predicted the strengths of the continuously cooled material as well as it fit the data for the isothermally cooled material.

The model was also able to successfully fit the KR_{10} toughness data for the isothermally treated samples (Figure 9), but the predictions of KR_{10} toughness for the continuously cooled samples were disappointing. The previously published analysis of this data had indicated

Table I. Estimated Values of Parameters in Equations Used to Predict Strength and Toughness

Yield strength	k_2 1.8026×10^{-8} S	k_3 1516.55 J/mole	k_4 869.56 K	k_5 102,390 J/mole
	σ_{max} 460.3 MPa	b_0 4899.3 MPa	b_1 −15.312 MPa/K	b_2 0.012498 MPa/K^2
KR_{10} toughness	m_2 2.284634×10^{-9} S			
	K_{max} (≤e633 °C) 67.45 MPa$\sqrt{m}$	c_0 176.844 MPa$\sqrt{m}$	c_1 −0.2185 MPa$\sqrt{m/K}$	
	(≥633 °C) 67.45 MPa$\sqrt{m}$	d_0 −104.368 MPa$\sqrt{m}$	d_1 0.2261 MPa$\sqrt{m/K}$	

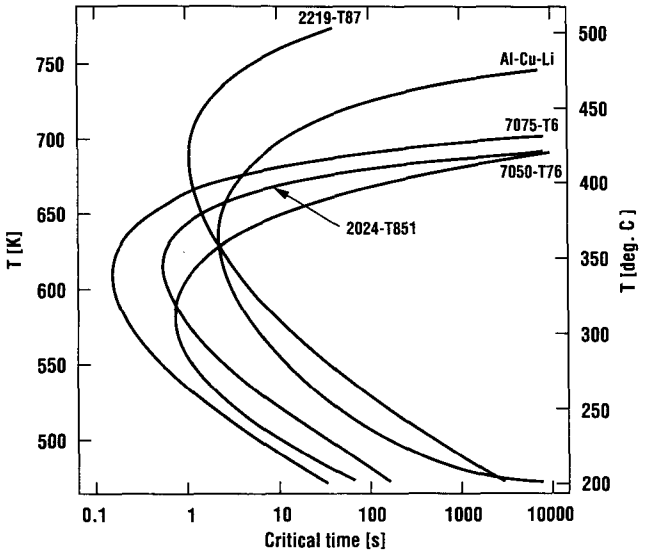

Fig. 5—Selected 0.995 yield strength TTP C-curves.

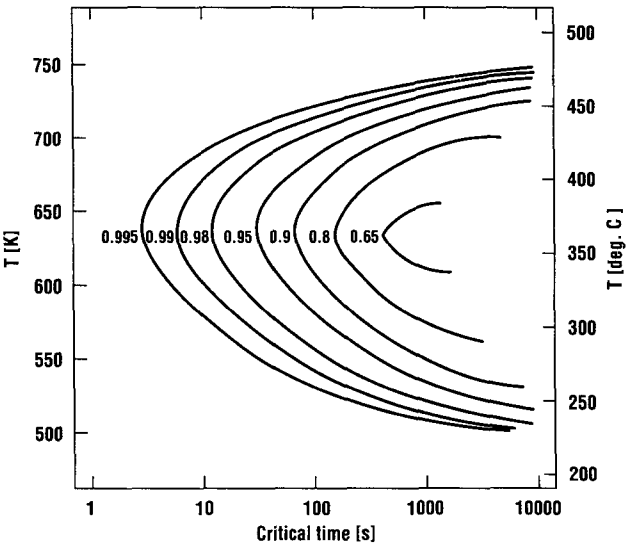

Fig. 7—C-curves for KR_{10} toughness.

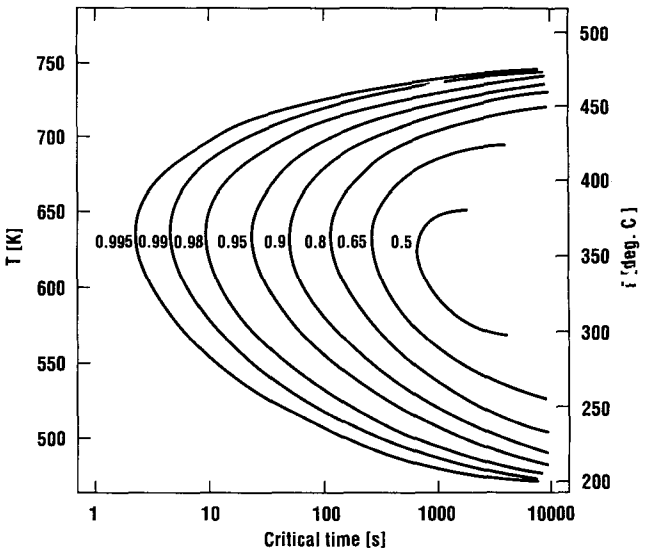

Fig. 6—TTP C-curves for yield strength.

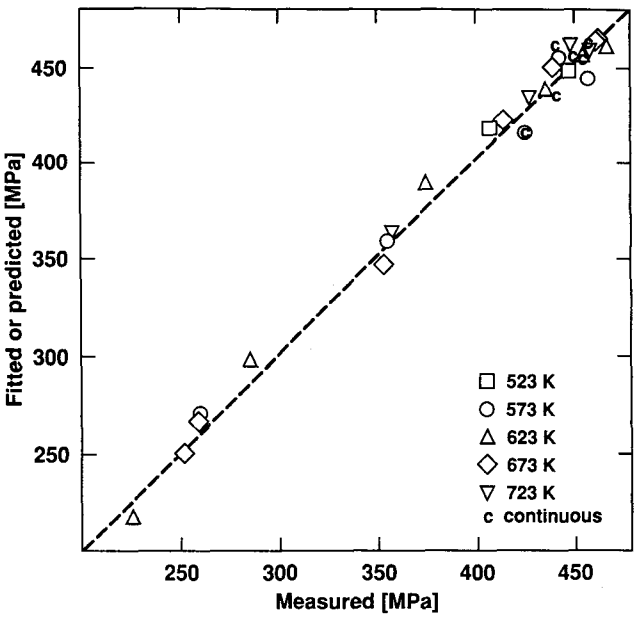

Fig. 8—Fitted (isothermal) or predicted (continuous cooling) values *vs* measured yield strength values.

that fracture toughness of continuously cooled material could apparently be predicted reasonably well from the cooling curve and a toughness TTP C-curve.[6] Results using the current model, however, were surprising because the errors in the present work (Table II) were greater.

Rigorous checking detected a procedural error in the previous work.[6,7] When the calculation error was rectified and new predictions made, the predictions using the newer model exhibited a slightly better fit with the data than those using the previous model. Both models are in many respects very similar, although the current model is more soundly based mathematically. The problem with the model is that it consistently overestimated the loss in the ability to develop toughness produced by slower quenching rates in different media (Figure 9). All the results from the continuous cooling studies, labeled C in Figure 9, consistently lie below the 45 deg. trend line established for the nominally isothermal studies. This behavior insures that predictions will always be conservative, and that feature makes it useful for most industrial applications. The sources of this error need to be examined carefully, however, to find out how to improve the model. Two possible sources of error are considered here: (1) the inter-relationship of strength and toughness; and (2) the influence on toughness of the size and distribution of the precipitates formed during cooling.

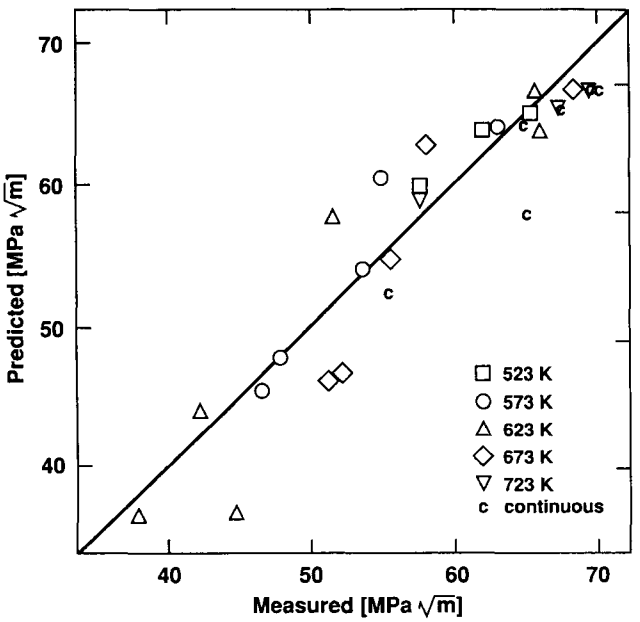

Fig. 9—Fitted (isothermal) and predicted (continuous cooling) values *vs* measured KR_{10} toughness values.

Table II. Measured and Predicted Values of KR_{10} for Continuously Quenched Materials

25 °C water	70.3 MPa$\sqrt{m}$	66.6 MPa$\sqrt{m}$
65 °C water	69.9	66.6
Glycol solution	67.5	65.2
100 °C water	65.0	64.0
Moving air	65.1	57.7
Still air	55.4	52.2

1. *The interrelationship of strength and toughness*

For all precipitation-hardened aluminum alloys, there is a tendency for the toughness of the product to increase as the strength falls due to an increase in the size of the "plastic zone" ahead of the crack.[14] There is also a tendency for toughness to fall with decreasing quench rate or increasing hold time during isothermal treatments because of an increase in the portion of intergranular fracture.[15] Because of the competing effects, the effect of decreasing quench rate on toughness usually follows a pattern: (1) decreases substantially with little loss in strength, (2) recovers to the level of rapidly quenched material as strength decreases, and (3) increases beyond this level as strength falls substantially.[14] For the material in this investigation, however, (and possibly for high strength Al-Li alloy products in general) toughness does not recover even after significant loss in strength. Therefore, the strength effect was not included in the model. Although the inter-relationship should be included in a general model to include material which shows a recovery and increase in fracture toughness with decreasing quench rate, omission in this model does not appear to be responsible for the overestimate in the loss in toughness. The reason for dismissing this explanation of the systematic error is that the model used the experimental data from the isothermal treatments to give the empirical parameters needed to predict the continuous cooling properties. Both sets of data (isothermal and continuous cooling) should be affected in rather similar ways by the inter-relationship, so the systematic overestimate by the model of the loss in toughness during continuous cooling is not readily explained by this inter-relationship. Isothermal hold temperature, however, had a strong effect on the combination of strength and toughness, as shown in Figure 10 which was obtained by cross plotting the fitted results of the isothermal studies. This observation indicates that the size and distribution of the

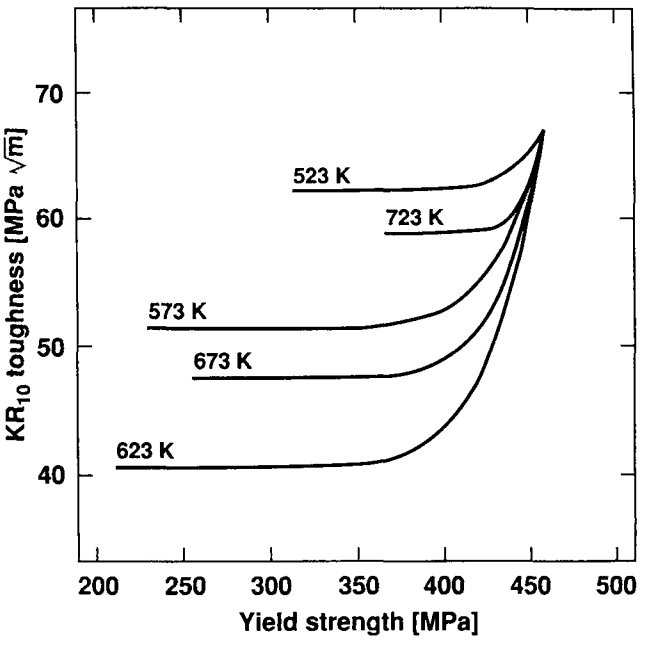

Fig. 10—Fitted properties.

precipitates formed during cooling, which are not considered directly in the model, have an effect which could be influential.

2. *The influence of the size and distribution of the precipitates*

The model is based on the loss in yield strength being linear with solute precipitated, and, thus, linear with respect to the total volume fraction, f_V, of precipitate. Vasudevan and Doherty have shown that loss of toughness due to grain boundary precipitates, at a constant strength level, is a function of the area fraction of precipitates on the grain boundary, $f_A(gb)$.[13] Making the simplifying assumption that the grain-boundary precipitates are spheres of radius r with an area density on the boundary of N_A, the succeeding immediately follows for the area and volume fractions on the boundary:

$$f_A(gb) = 4\pi r^2 N_A$$

$$f_V(gb) = 4\pi r^3 \frac{N_A}{3}$$

so

$$f_A(gb) = 3\,\frac{f_v(gb)}{r} \qquad [10]$$

The reciprocal dependence, Eq. [10], of grain-boundary area fraction on precipitate size will be found for any precipitate shape including the platelike shapes of the grain-boundary T_1 precipitate seen in this study. The reciprocal dependence of area fraction, and thus toughness loss, on precipitate size can immediately account for the greater loss of toughness at fixed loss in strength as hold temperature falls from 723 to 623 K (Figure 10). Grain-boundary precipitates were seen to be smaller and more closely spaced as the isothermal-treatment temperature decreased. However, the reversal of this trend, giving smaller losses in toughness at a constant loss in strength, as the isothermal-treatment temperature fell from 623 to 523 K (Figure 10), clearly indicates that some other factor must be influencing the loss in toughness. That factor appears to be the precipitates within the grain. With the decreasing isothermal-treatment temperature, the amount of T_B precipitates within the grain increased and Θ' began to precipitate in the matrix. Therefore, for a particular strength (influenced by loss of solute through precipitation of T_B and T_1 and Θ' and by the strengthening effect of Θ'), the loss in toughness of material held below 623 K would be less than that of material held at 623 K, because at the lower temperatures, more of the precipitate would be within the grains and less in the boundaries.

These ideas can explain, qualitatively, the observed temperature dependence of the relative loss of toughness and yield strength. They do not directly explain, however, the systematic error in the model which led to conservative predictions of the toughness after continuous cooling at low-average quench rates. If the precipitation during isothermal treatments and continuous cooling had produced the same effects, the model should be valid, irrespective of the temperature effect. This line of reasoning suggests that the size and distribution of the precipitates formed during continuous cooling may not be that assumed in a model based solely on isothermal precipitation. Precipitation, a nucleation and growth process, is very likely to give rather different precipitate distributions when the temperature is lowered continuously as compared to isothermal treatments. The nuclei formed at high temperatures would be expected to modify the subsequent kinetics and sites for nucleation at lower temperatures.[16] This effect is presented schematically in Figure 11. An examination of continuously quenched samples revealed a wide range of precipitate sizes on the boundaries and within the grains, but a conclusion could not be drawn regarding effects of prior precipitation on precipitation kinetics and morphology during continuous cooling.[7] Simple two-step or three-step isothermal treatments would provide an opportunity to confirm that precipitates formed at lower temperatures had different distributions than those formed by directly quenching to the lower temperature. Unfortunately, the desirability of this experimental approach was not realized until after all of the experimental material had been disposed of. Consequently, new material in a further study will have to be used to test this concept.

CONCLUSIONS

A new model based on a more mathematically rigorous method than previous models improves the ability to predict the capacity of precipitation-hardenable–aluminum alloy products to develop strength after arbitrary cooling conditions.

The model progressively underestimated the ability to develop toughness as the cooling rate decreased. For industrial purposes, this conservative estimate is adequate for materials such as Al-Li alloy products which do not recover toughness with a decreasing quench rate after an initial loss.

The reason why the model underestimated the ability to develop toughness is attributed to precipitation at higher temperatures having an effect on the size and distribution of precipitates formed at lower temperatures. Therefore, effects of precipitation during isothermal treatments cannot be used to predict effects of precipitation during continuous cooling. Detailed metallographic investigations of simple multistep quenches are proposed to provide the basis for a model which takes this factor into account.

APPENDIX A

Derivation of Equation [7]

In this Appendix, we rigorously show that, we can substitute $1/C_i(T)$ for $k(T)$ in Eq. [4] to produce Eq. [7]. Although this may be obvious, both the methodology of formally doing it, as well as some of the results, will be used in Appendix B to develop a much more complex Eq. [8].

To visualize the derivation, assume a three-step cooling curve presented in Figure A1 where the material is quenched instantaneously to and from each isothermal hold. Using notations from the main body of the article and Eq. [5], the following can be written for the first isothermal segment of the cooling curve:

$$\sigma_1 = \sigma_{\min}(T_1) + (\sigma_{\max} - \sigma_{\min}(T_1)) \exp\left(-\frac{\Delta t_1}{C_i(T_1)}\right) \qquad [A1]$$

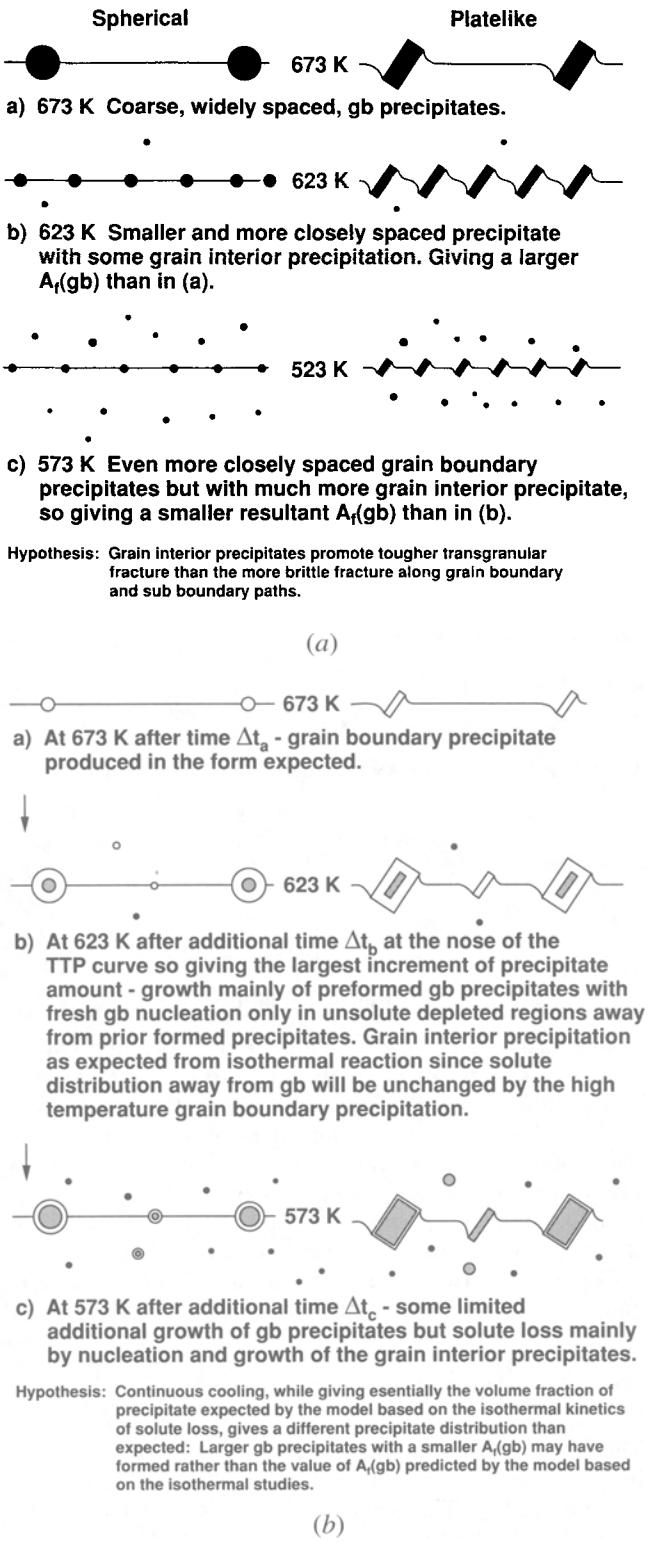

Fig. 11—(*a*) Schematic of isothermal precipitation at three temperatures to the same total volume fraction, V_f, precipitated; and (*b*) postulated precipitation morphology during continuous cooling with increasing volume fraction, V_f, precipitated.

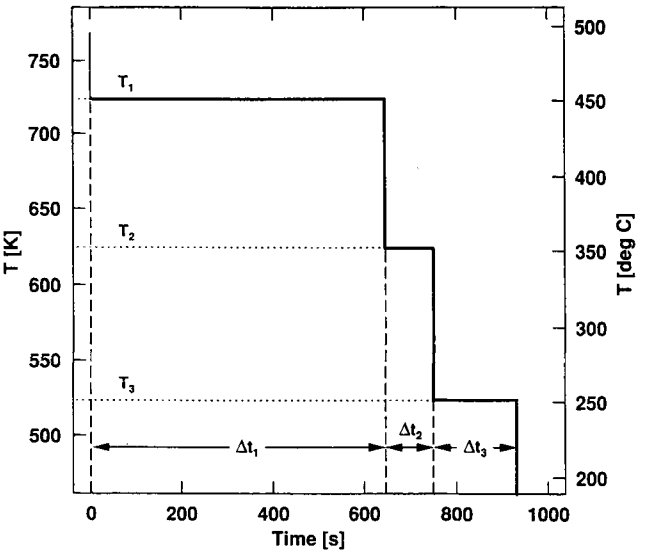

Fig. A1—Three-step cooling curve.

where σ_1 = value of property σ after time Δt_1 at temperature T_1.

After the first isothermal hold, the material is quenched to temperature T_2 and held for time Δt_2. Thus,

$$\sigma_1 = \sigma_{\min}(T_2) + (\sigma_{\max} - \sigma_{\min}(T_2)) \exp\left(-\frac{\tau_1}{C_t(T_2)}\right) \quad [A2]$$

where τ_1 = "equivalent time" for temperature T_2, *i.e.*, the time necessary to attain a value of σ_1 at temperature T_2 instead of T_1.

Now the following expression for σ_2 can be written:

$$\sigma_2 = \sigma_{\min}(T_2) + \left[(\sigma_{\max} - \sigma_{\min}(T_2)) \exp \cdot\left(-\frac{\tau_1}{C_t(T_2)}\right)\right] \exp\left(-\frac{\Delta t_2}{C_t(T_2)}\right) \quad [A3]$$

Individual pieces of the σ trajectory, together with the symbols used, are shown in Figure A2(a). The whole trajectory is shown in Figure A3(a).

Comparing Eqs. [A2] and [A3] we can obtain

$$\sigma_2 = \sigma_{\min}(T_2) + (\sigma_1 - \sigma_{\min}(T_2)) \exp\left(-\frac{\Delta t_2}{C_t(T_2)}\right) \quad [A4]$$

which is identical with Eq. [A1] if we shift time by one segment to the right on the cooling curve. Using an identical argument, one can obtain

$$\sigma_3 = \sigma_{\min}(T_3) + (\sigma_2 - \sigma_{\min}(T_3)) \exp\left(-\frac{\Delta t_3}{C_t(T_3)}\right) \quad [A5]$$

and it follows that

$$\sigma_i = \sigma_{\min}(T_i) + (\sigma_{i-1} - \sigma_{\min}(T_i)) \exp\left(-\frac{\Delta t_i}{C_t(T_i)}\right) \quad [A6]$$

Equation [A6] indicates that the property loss for a given isothermal segment of the cooling curve depends only on the current "driving force," $\sigma_{i-1} - \sigma_{\min}(T_i)$, and

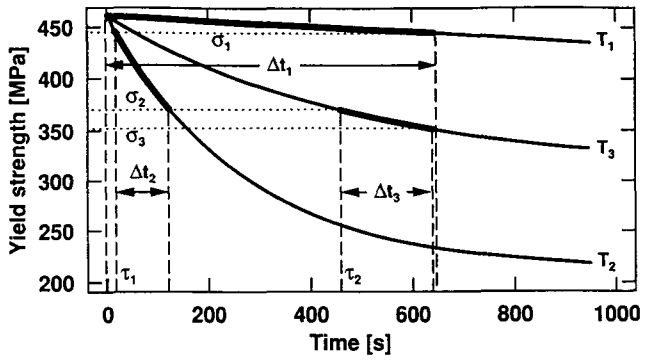

(*a*)

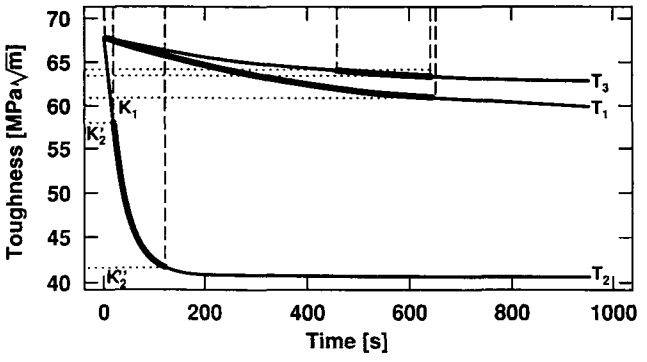

(*b*)

Fig. A2—Pieces of σ and K trajectories.

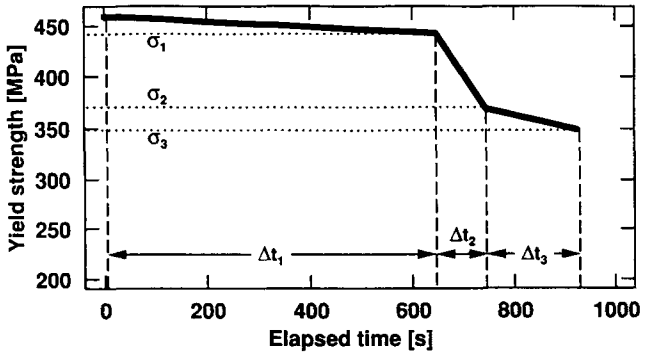

(*a*)

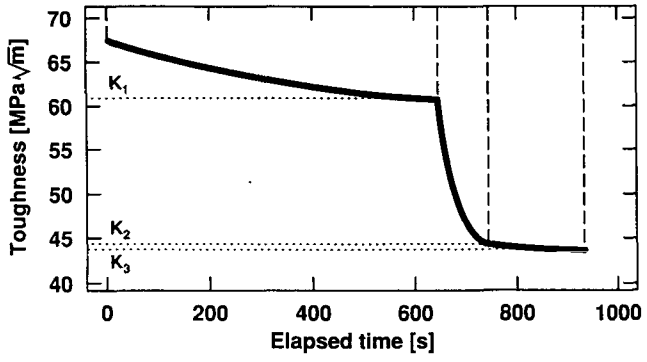

(*b*)

Fig. A3—σ and K trajectories.

not on the path which was used to get to the current point. This is simply another way of stating the first-order assumptions.

After subtracting σ_{i-1} from both sides of Eq. [A6] and rearranging, one can obtain

$$\Delta\sigma_i = (\sigma_{i-1} - \sigma_{\min}(T_i))\left(\exp\left(-\frac{\Delta t_i}{C_t(T_i)}\right) - 1\right) \quad [A7]$$

where $\Delta\sigma_i = \sigma_i - \sigma_{i-1}$

Now, the exponential function can be expanded into the Taylor expansion

$$\exp(-x) = 1 - x + o(x)$$

where the function $o(x)$ has the following property:

$$\lim_{x\to 0}\left(\frac{o(x)}{x}\right) = 0$$

Using this expansion in Eq. [A7], we get

$$\frac{\Delta\sigma_i}{\Delta t_i} = (\sigma_{i-1} - \sigma_{\min}(T_i))\left(-\frac{1}{C_t(T_i)} + \frac{o(\Delta t_i)}{\Delta t_i}\right) \quad [A8]$$

and passing to the limit as $\Delta t_i \to 0$ produces

$$\frac{d\sigma}{dt} = -\frac{1}{C_t(T)}(\sigma - \sigma_{\min}(T)) \quad [A9]$$

which is Eq. [7] and is identical to Eq. [4] with

$$k(T) = \left(\frac{1}{C_t(T)}\right)$$

APPENDIX B

Derivation of Equation [8]

The basic idea of the toughness model is to use equivalent times from the strength model to calculate successive increments of K. The three-step cooling curve from Figure A1 is used, along with Figure A2(a) which shows the elements of the σ trajectory and Figure A2(b) which gives the corresponding elements of the K trajectory in such a way that the time axes are common. The whole K trajectory is shown in Figure A3(b).

For the first isothermal segment at T_1, the value of K can be calculated in exactly the same way as for σ:

$$K_1 = K_{\min}(T_1) + (K_{\max} - K_{\min}(T_1))\exp\left(-\frac{\Delta t_1}{D_t(T_1)}\right) \quad [B1]$$

The value of potential toughness used as the starting value in the second step at T_2 is, however, K_2' not K_1 (Figure A2(b)). This value is the one calculated for the equivalent time of τ_1 at T_2 that would give the same potential strength at T_2, as would correspond to the solute remaining in solution after the first time step, Δt_1 at T_1. This strength is σ_1. The basis for the choice of K_2' not K_1 for the starting value of toughness for the second step is the assumption that the loss of toughness at T_2 is determined by the solute that will precipitate at this temperature during holding for a time Δt_2 and not by the

current value of toughness, K_1, that is determined by the amount and distribution of solute previously precipitated:

$$K_2' = K_{min}(T_2) + (K_{max} - K_{min}(T_2)) \exp\left(-\frac{\tau_1}{D_t(T_2)}\right) \quad [B2]$$

From that point, we move along the T_2 isotherm for time Δt_2 obtaining K_2'', as written

$$K_2'' = K_{min}(T_2) + (K_{max} - K_{min}(T_2)) \exp\left(-\frac{\tau_1}{D_t(T_2)}\right) \exp\left(-\frac{\Delta t_2}{D_t(T_2)}\right) \quad [B3]$$

The loss in toughness accrued at temperature T_2 is equal to

$$\Delta K_2 = K_2'' - K_2' = K_{min}(T_2) + (K_{max} - K_{min}(T_2)) \exp\left(-\frac{\tau_1}{D_t(T_2)}\right)\left[\exp\left(-\frac{\Delta t_2}{D_t(T_2)}\right) - 1\right] \quad [B4]$$

However, from Eq. [A2] we get

$$\exp(-\tau_1) = \left[\frac{\sigma_1 - \sigma_{min}(T_2)}{\sigma_{max} - \sigma_{min}(T_2)}\right]^{C_t(T_2)}$$

and simple substitution produces

$$\Delta K_2 = (K_{max} - K_{min}(T_2)) \left[\frac{\sigma_1 - \sigma_{min}(T_2)}{\sigma_{max} - \sigma_{min}(T_2)}\right]^{C_t(T_2)/D_t(T_2)} \cdot \left[\exp\left(-\frac{\Delta t_2}{D_t(T_2)}\right) - 1\right] \quad [B5]$$

An identical argument can be used to obtain ΔK_3 and similarly to the development for σ we get by induction:

$$\Delta K_i = (K_{max} - K_{min}(T_i)) \left[\frac{\sigma_{i-1} - \sigma_{min}(T_i)}{\sigma_{max} - \sigma_{min}(T_i)}\right]^{C_t(T_i)/D_t(T_i)} \cdot \left[\exp\left(-\frac{\Delta t_i}{D_t(T_i)}\right) - 1\right] \quad [B6]$$

Finally, by expanding the exponential, dividing by Δt_i, and passing to the limit as $\Delta t_i \to 0$, we obtain

$$\frac{dK}{dt} = -\frac{1}{D_t(T)}(K_{max} - K_{min}(T)) \left[\frac{\sigma - \sigma_{min}(T)}{\sigma_{max} - \sigma_{min}(T)}\right]^{C_t(T)/D_t(T)} \quad [B7]$$

which is identical to Eq. [8].

ACKNOWLEDGMENTS

The authors acknowledge the contribution of O. Richmond for suggesting that the kinetics of the loss in strength be structured in the form of a differential equation. The assistance of W.R. Vogt with the experimental portion of this work and that of E.A. Ludwiczak, J.J. Ptasienski, and J.C. Casato with the structural analysis is also gratefully acknowledged. The authors thank the Aluminum Company of America for permission to publish.

REFERENCES

1. J.W. Cahn: *Acta Metall.*, 1956, vol. 4, pp. 572-75.
2. J.W. Evancho and J.T. Staley: *Metall. Trans.*, 1974, vol. 5, pp. 43-47.
3. J.T. Staley: *Mater. Sci. Technol.*, 1987, vol. 3, pp. 923-35.
4. J.W. Cahn: *Acta Metall.*, 1956, vol. 4, pp. 449-59.
5. L. Swartzengruber, W. Boettinger, L. Ives, S. Coriell, P. Blau, J. Cahn, and R. Mehrabian: *Report No. NBSIR 80-2069*, National Bureau of Standards, Washington, D.C., 1980.
6. J.T. Staley and R.D. Doherty: *Proc. 5th Int. Al-Li Conf.*, Williamsburg, VA, March 27–31, 1989, Materials and Component Engineering Publications Ltd., Birmingham, UK, vol. 1, pp. 345-54.
7. J.T. Staley: Ph.D. Thesis, Drexel University, Philadelphia, PA, 1989.
8. E.A. Ludwiczak and R.J. Rioja: *Scripta Metall.*, 1991, vol. 25, pp. 1415-19.
9. M.H. Tosten, A.K. Vasudévan, and P.R. Howell: *Metall. Trans. A*, 1988, vol. 19A, pp. 51-66.
10. A. Hindmarsh: in *Scientific Computing: Proc. IMACS World Congress on Systems, Simulation, & Scientific Computation*, R.S. Stepleman, M. Carver, R. Peskin, W.S. Ames, and R. Vichnezetsky, eds., North-Holland, Amsterdam, 1983, pp. 136-48.
11. J. Dennis, D. Goy, and R. Welsch: *ACM Trans. Math.*, 1981, vol. 7, pp. 349-68.
12. L.K. Ives, L.J. Swartzendruber, W.J. Boettinger, M. Rosen, S.D. Ridder, F.S. Biancaniello, R.C. Reno, D.B. Ballard, and R. Mehrabian: *Report No. NBISR 83-2669*, National Bureau of Standards, Washington, D.C., 1983.
13. A.K. Vasudevan and R.D. Doherty: *Acta Metall.*, 1987, vol. 35 (6), pp. 1193-219.
14. J.T. Staley: *ASTM STP 605*, ASTM, Philadelphia, PA, 1975, pp. 75-96.
15. G.N. Colvin and E.A. Starke, Jr.: *SAMPE Q.*, 1988, vol. 19 (4), pp. 10-21.
16. R.D. Doherty: in Part 2 *Physical Metallurgy*, R.W. Cahn and P. Haasen, eds., North-Holland, Amsterdam, 1983, pp. 933-1030.